ELSEVIER

Journal of Nuclear Materials 254 (1998) 65–73

journal of nuclear materials

Effect of physical vapor deposition on microstructure and properties of uranium–6 wt% niobium alloy

A.J. Sunwoo *, T.S. Chow, C.J. Long

Lawrence Livermore National Laboratory, 7000 East Avenue, Livermore, CA 94550, USA

Received 6 January 1997; accepted 13 August 1997

Abstract

Uranium–6 wt% niobium alloy samples produced by the physical vapor deposition (PVD) process reveal unique metallurgical and mechanical properties. From two deposition conditions at 580°C with a bias voltage, and at 900°C without bias, the microstructural characterization indicates that the grain distribution morphology of the alloy in each case was primarily determined by the deposition process. Applying the bias voltage of 500 V during the PVD changed the grain morphology from a typical columnar to an equiaxed structure. On the other hand, the substrate temperature controlled the diffusivity of Nb and U and hence the characteristic 'banding' into slightly different compositions observed in such microstructures. Very fine, equiaxed grains of the 580°C specimens are mainly responsible for the highly favorable strength and ductility combination. However, the columnar structure morphology present in the 900°C specimens did not adversely affect the tensile behavior. The 580°C material exhibited superior subzero tensile properties compared to both the 900°C and the wrought-processed materials. The PVD materials that had been specifically heat treated after deposition had room temperature tensile properties comparable to the wrought-processed material. © 1998 Elsevier Science B.V.

1. Introduction

The physical vapor deposition (PVD) process for producing the uranium–6 wt% niobium (U–6% Nb) alloy is being developed as a potential alternative to the conventional wrought processing. This alternative processing study is motivated by the need to improve the efficiency in quantity of material actually used from each production process and to reduce the cost of fabrication.

Long et al. [1] were the first to demonstrate successfully the feasibility of producing a high purity, fully dense U–6% Nb alloy using the electron beam PVD processing. Subsequent heat treatment of this material yielded samples with tensile properties comparable to those of the wrought-processed material. Alloys produced with the PVD process exhibit a great potential for the applications that require strength, ductility, and corrosion resistance. However, in order to optimize the PVD process, it is important to understand the mechanisms that control the microstructure and thereby the deformation behavior. The purpose of this work was to determine the effect of the PVD process conditions on the microstructure and mechanical properties of the U–6% Nb alloy, and to compare the mechanical property features with those of the wrought-processed material.

2. Experimental procedure

A schematic sketch of PVD experimental setup is shown in Fig. 1. The setup consisted of an electron beam gun, a bottom-fed water-cooled crucible, an enclosure containing thermally controlled substrates, and a water-cooled vacuum chamber. As the overhead electron beam melts the U–6% Nb feedstock ingot, the U and Nb vaporize and coat the substrates which are mounted 11.3° and 13° off centerline. Uranium evaporation rate was under closed loop control during deposition. Probe lasers were tuned to monitor the densities of the U and Nb vapors. Uranium density was used in a feedback loop to control the electron beam power. Niobium density was monitored but not controlled. Video images of the melt were digitally

* Corresponding author. E-mail: sunwoo1@poptop.llnl.gov.

PII S0022-3115(97)00296-1

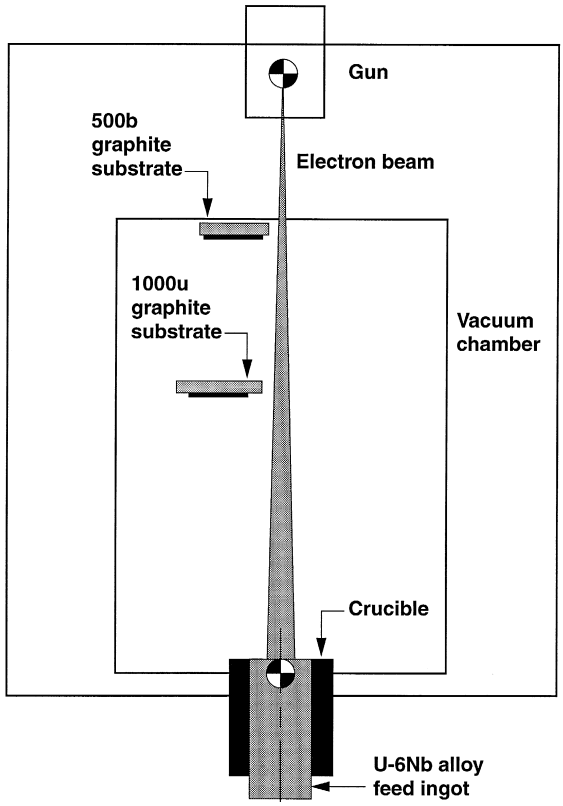

Fig. 1. A schematic of PVD process setup.

processed to determine the melt level, which was then used in a feedback loop to control the feed rate.

The feedstock ingot was made initially by electron beam cold hearth melting and casting of a U–6% Nb alloy available from a previous wrought-processed. It is assumed that the ingot chemistry was within Nb limits of 5.2 and 6.5 wt% and that there was no loss of Nb through vaporization. The bulk composition of the PVD samples was analyzed using atomic emission spectroscopy (AES) and the results are listed in Table 1.

The vapor deposition conditions are summarized in Table 2. Samples were obtained as solidified deposits on graphite substrates A and B following 17 h of continuous operation in vacuum ($\sim 10^{-5}$ Torr). The substrates were electrically insulated to impose a bias voltage. At the operating electron-gun current of 5.5 A, the background

Table 1
Analyzed chemical composition of PVD U–6Nb alloy using atomic emission spectroscopy

Sample ID	Nb (wt%) mini/max	U (wt%) minimum
Specification	5.2/6.5	93
500b	6.5 ± 0.1	balance
1000u	5.1 ± 0.1	balance

Table 2
Summary of PVD parameters

Electron beam power (kW)	185
Vapor rate (kg/h)	5.1
Shutter open (h)	17
Ingot feed (kg)	95
Substrate A (500b)	graphite
Temperature (°C)	580
Voltage (V)	500
Thickness (mm)	2.2
Vapor flux ($g/h/cm^2$)	0.53
Substrate B (1000u)	graphite
Temperature (°C)	900
Voltage (V)	none
Thickness (mm)	5.08
Vapor flux ($g/h/cm^2$)	1.2

ion fraction was calculated to be 2%. Substrate A, identified as 500b, was produced at 580°C with bias imposed on the substrate ranging from 0.15 to 0.5 kV and with 2% ionization. Substrate B, identified as 1000u, was produced at 900°C without bias. The particular PVD conditions were chosen to determine the beneficial effect of ion bombardment, if any, on modulating the deposited microstructure. Evaluation of the results would then allow the use of an appropriate substrate temperature for best system operation. Another difference was the substrate location relative to the vapor source; the deposition rate of the 500b was about 50% that of the 1000u, resulting in a much thinner plate. The final dimensions of the as-deposited plates of 500b and 1000u were 10.7 cm × 12.2 cm × 0.2 cm and 10.2 cm × 30.5 cm × 0.5 cm, respectively.

In order to reproduce the conditions used for wrought material, the as-deposited materials were machined into flat, dogbone-shaped tensile specimens. To ensure that failure occurred within the gage length, the gage thickness was thinned from 2.3 mm to 1.5 mm. Subsequently, the samples were vacuum solution heat treated for 3 h at 800°C, followed by quenching in water. A set of both 500b and 1000u specimens was also aged at 200°C for 2 h in vacuum. After the heat treatments, both the 500b and 1000u specimens were characterized for composition, microstructure, and tensile properties. For optical microscopy, metallographic samples were prepared using a standard polishing technique, followed by electroetching in 1:1 orthophosphoric acid:water. Vickers microhardness measurements were made through the thickness on the polished surface of heat treated PVD samples. All tensile specimens were pulled to failure with a constant crosshead travel of 1.27 mm/min (an initial strain rate of $\sim 10^{-3}$/s) at 25°C; only the aged specimens were tested at −40°C. Two extensometers were used to obtain average strain data. The test matrix was chosen to attain a comprehensive overview of the PVD material characteristics. However, because of the limited number of specimens available, a

single specimen was tested for each condition. In the case of an anomaly from the expected trend, the test condition was retested to ensure reproducibility. Scanning electron microscopy (SEM) was employed to examine the fracture surfaces.

3. Results and discussion

3.1. Effect of phases present in the U-6% Nb alloy

The results of AES analysis on the as-deposited samples and the material specification limits are listed in Table 1. The bulk Nb contents for 500b and 1000u were at the Nb maximum (6.5 wt%) and minimum (5.1 wt%), respectively. The available phase diagram of U–Nb alloy system is shown in Fig. 2 [2]. The diagram indicates that U containing 6 wt% Nb alloy undergoes an eutectoid phase transformation at 647°C, from a single phase gamma (γ) to a two-phase mixture of alpha (α'') and gamma (γ°) [3,4]. However, Nb is purposely added to U to improve its corrosion resistance, and is only beneficial if it remains in solid solution. To ensure this, a typical heat treatment used for the alloy is to equilibrate Nb in the γ phase, followed by water quenching to room temperature. This causes the γ phase to transform martensitically to a Nb supersaturated variant of the α phase [5,6]. The alloy is then aged for 2 h at 200°C to precipitate small amounts of the Nb phase in the martensitic α matrix. The subsequent aging allows the alloy to gain some strength without much loss of its corrosion resistance, or ductility. Thus, the 500b and 1000u specimens were heat treated in the same fashion in order to eradicate the post PVD effects, and to establish a comparison between the PVD and wrought processes.

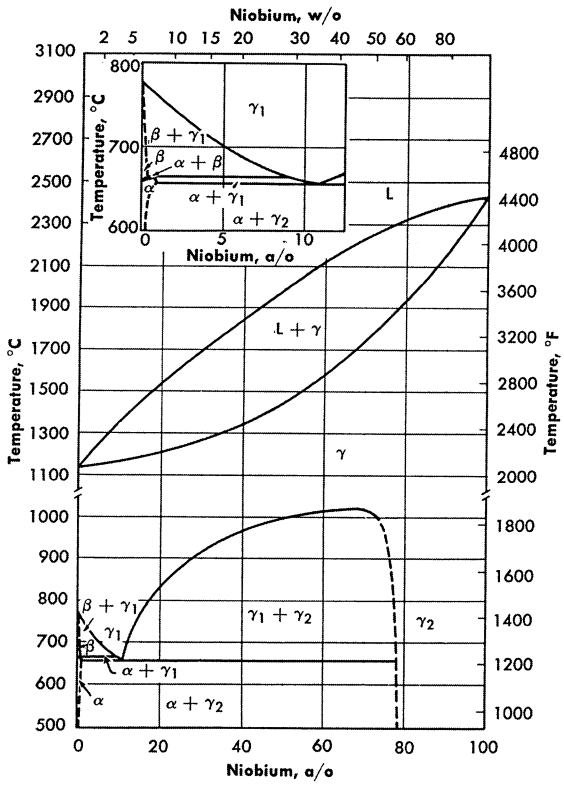

Fig. 2. The phase diagram of U–Nb alloy system.

3.2. Effect of temperature on microstructure

The effects of the PVD temperatures on the microstructure of heat treated 500b and 1000u are shown in Fig. 3(a) and (b), respectively; note the difference in the micron markers. The composite micrographs of two samples revealed distinctly different grain sizes and morphology. Both materials appeared to be free of any visible inclusions. The 500b sample contained very fine, mainly equiaxed grains that showed only very slight growth directionality (Fig. 3(a)). It appears that in the case of 500b, being deposited in a two-phase region, the process has restricted the grain growth to a grain size of about 20 μm. On the other hand, the microstructure of 1000u was dramatically different (Fig. 3(b)). The grains were predominantly columnar, as a result of a preferred growth direction. In the 1000u sample, U and Nb were deposited into a single-phase region at the substrate temperature close to 0.75 of the absolute melting temperature. As a result, grain boundaries are highly mobile during deposition. The width of the columnar grains was about a factor of 2 larger than the grain diameter in 500b.

The other discernible difference revealed in the micrographs is the formation of bands through the thickness. It is well known that Nb tends to diffuse rather slowly in U [1]. If one considers the PVD temperatures and the diffusivity of Nb in U as the controlling factors that have contributed to the formation of the observed microbands, then a simple calculation of Nb diffusion in U using $D_0 = 1.5 \times 10^{-4}$ cm^2/s and $Q = 33$ kcal/mol shows that after 17 h at 580°C, Nb would have diffused only 1.7 μm, compared to 25 μm after 17 h at 900°C. Thus, the diffused bands seen in 1000u are the results of a partial homogenization of Nb within gamma U. The band width from peak-to-peak was measured to be about 100 μm in 1000u, and about 40 μm in 500b. Another microstructural anomaly unique to this particular series of the 1000u samples was the presence of intergranular microvoids found in parts of the Nb-lean regions.

[1] Uranium–6 niobium alloy, Dow Rocky Flats Materials Datasheets RFP-1613 (1971).

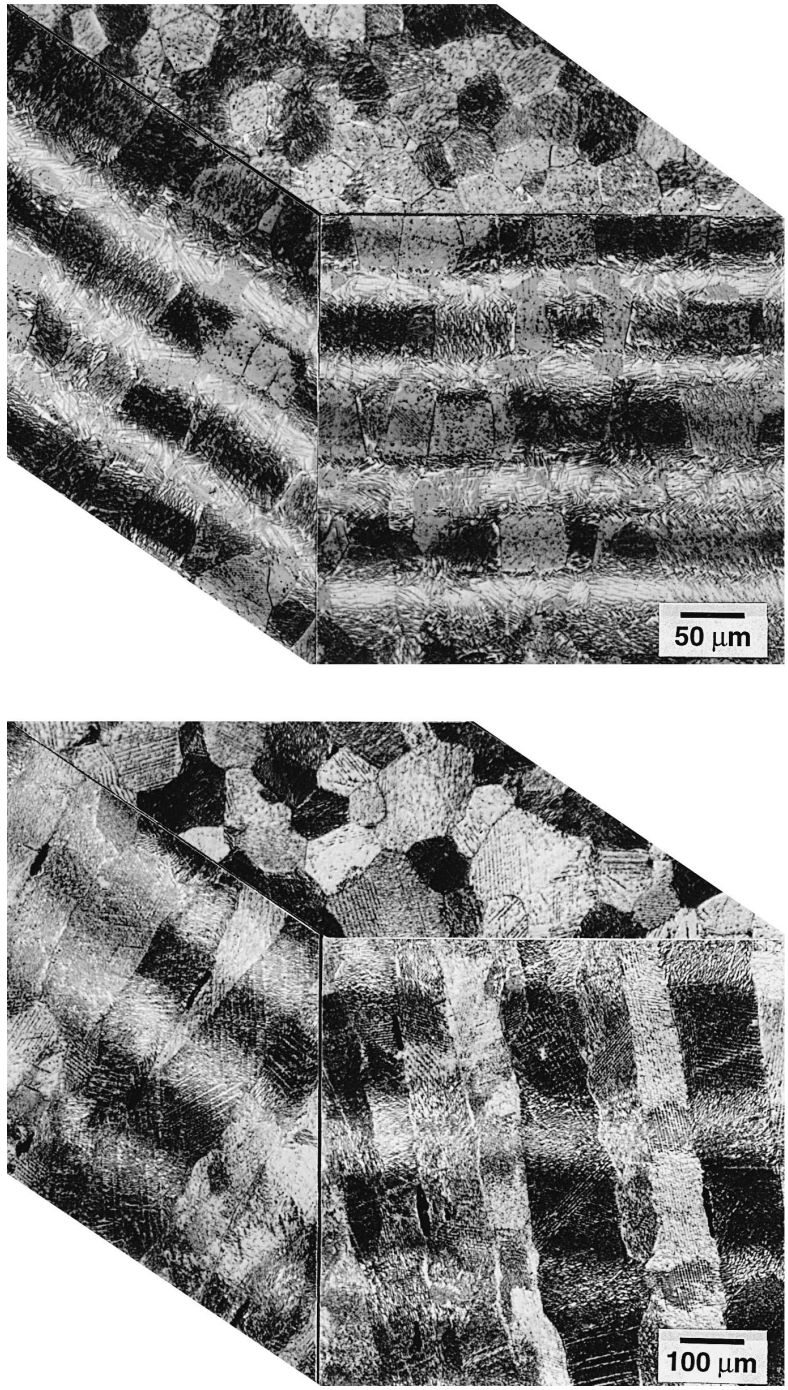

Fig. 3. Composite micrographs of PVD materials, showing the effects of temperature and bias on the microstructure: (a) 500b produced at 580°C with bias; (b) 1000u produced at 900°C with no bias.

3.3. Effect of composition on microhardness

Fig. 4 displays the variations of Nb content through the thickness of the samples and its effect on microhardness. In order to correlate the Nb content in the microbands to microhardness, energy dispersive spectroscopy (EDS) was used. The average Nb concentration in Nb-rich regions of 500b was close to 9%, with one Nb-rich region exceeding

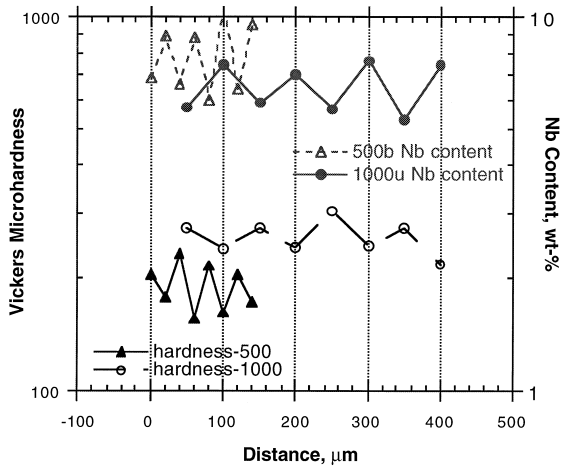

Fig. 4. A correlation between Nb concentration and Vickers microhardness for 500b and 1000u materials.

10%, and the average Nb concentration in Nb-lean regions was about 6.5%. For 1000u, the banding of Nb was not as severe as the 500b and the Nb concentration averaged about 6.5%. Although the EDS values are higher than analyzed by AES, the general trend is consistent, where the lower Nb content of 1000u could be attributed to a lower bulk Nb content.

When Vickers microhardness measurements and Nb concentrations are plotted with respect to microbanding in 500b and 1000u samples, the figure shows the similarities as well as the differences between the two PVD materials (Fig. 4). The Nb-rich regions were consistently softer than the Nb-lean regions. In comparison to 500b, the difference in hardness values reported between the rich and the lean regions in 1000u was more moderate, and for a relatively similar Nb concentration in the Nb-lean regions, the overall hardness of 1000u was significantly higher. It appears that not only does the grain size and morphology influence the hardness, but also the Nb concentration, as expected.

3.4. Effect of bias

The equiaxed grain morphology and higher Nb content in the Nb-rich microbands seen in 500b are most likely connected to the effects of an applied bias. Imposition of a biased voltage during the PVD process would cause ion bombardment with a greater kinetic energy than that with ions without the applied bias. Hence, the possible effects

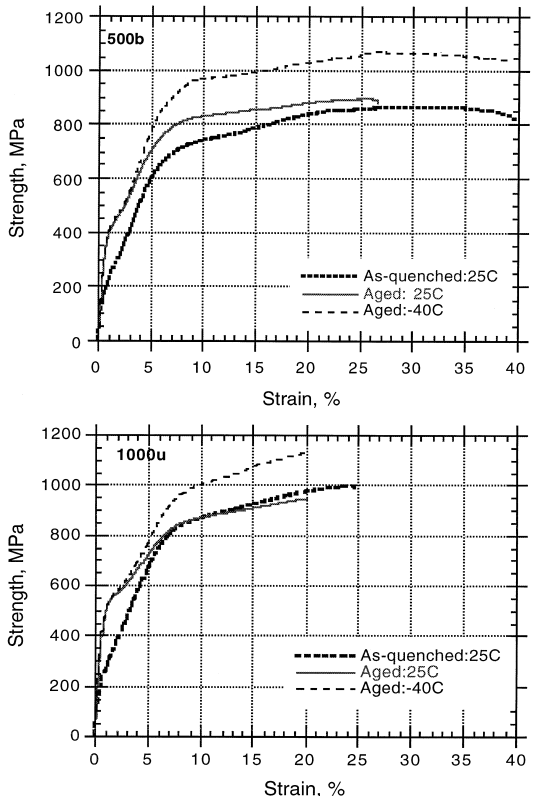

Fig. 5. The effect of PVD conditions, heat treatments, and test temperatures on the tensile deformation behavior of 500b and 1000u.

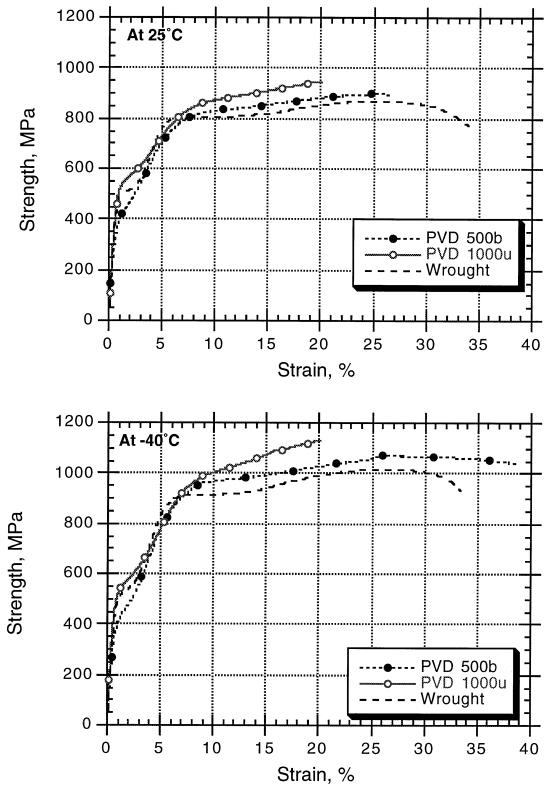

Fig. 6. The effect of processing and test temperatures on the tensile deformation behavior of PVD and wrought-processed U–6Nb alloy.

of ion bombardment at the interface are likely to be of several kinds. First, bombardment could generate a localized heating at the interface and, followed by an instantaneous cooling to the substrate temperature of 580°C, it could promote either a phase transformation, or a nucleation event [7]. Second, it could generate collision cascades either to disrupt the columnar formation, or to develop the banding structure. As indicated by the microhardness results and Nb content correlation, the Nb-lean bands tend to be harder, and hence the ability to penetrate the deposited layer will depend on the energy of the ions. One envisions the following effects to occur. Uranium has a higher vapor pressure than Nb so the initial deposited layer would be U [8]. As the U layer thickens, the softer Nb ions have difficulty penetrating the U layer and start building a Nb-enriched layer, until the U ions bombard and penetrate into the Nb-rich layer to start another U-enriched layer. Concurrently, the substrate temperature allows some self-diffusion of U and Nb, and the post heat treatment helps to partially homogenize Nb into the γ phase.

3.5. Tensile behavior

Fig. 5(a) and (b) show the stress–strain curves of 500b and 1000u, respectively, tested at 25°C and −40°C. In the as-quenched condition, both the 500b and 1000u speci-

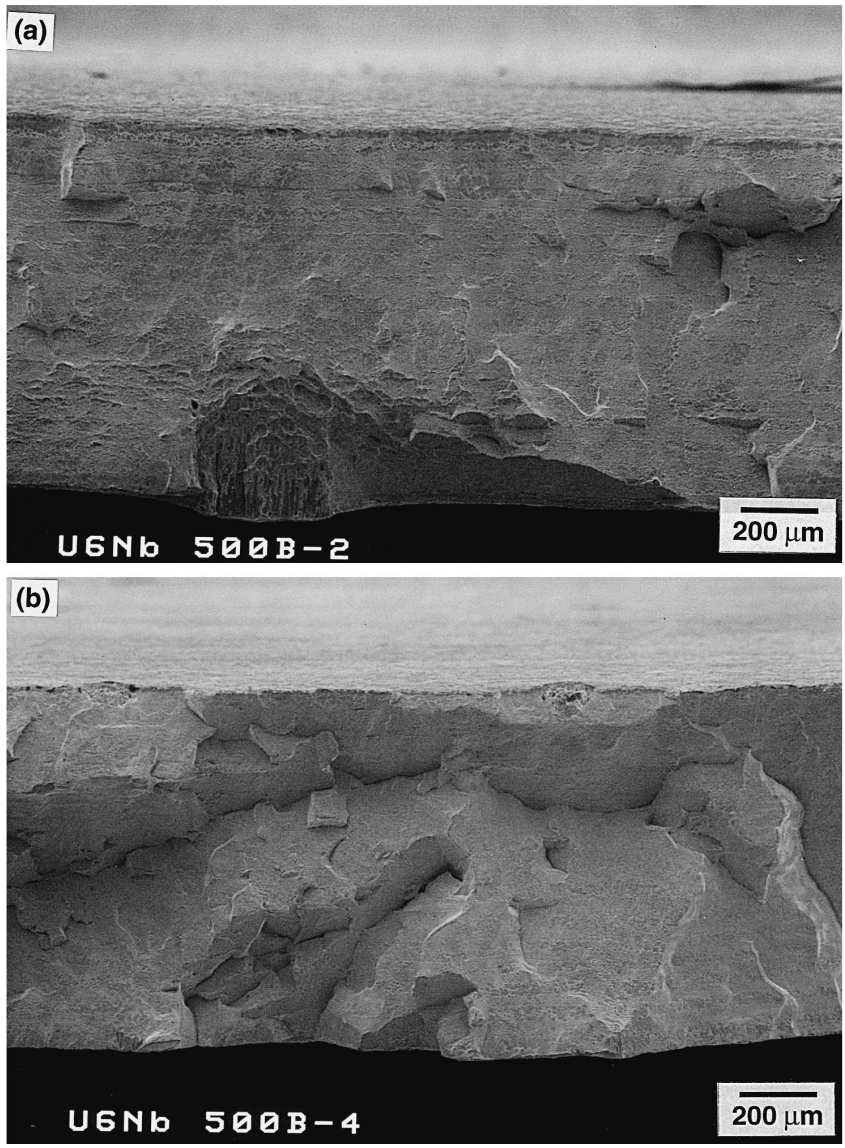

Fig. 7. SEM fractography of gamma quenched and aged 500b specimens, showing the effects of test temperature on deformation: (a) tested at 25°C; (b) tested at −40°C.

mens did not exhibit the 'easy flow' characteristics that are typical of the wrought U–6% Nb alloy [9,10]; instead, they displayed deformation behavior that was somewhat closer to 'conventional' metallic materials. If one presumes that the yielding occurs at the onset of plasticity, (rather than using the conventional method of determining the yield strength, 0.2% offset), then the 500b specimens displayed an excellent combination of strength and ductility, deforming beyond plastic instability to about 40% elongation. In comparison, the 1000u specimens exhibited similar yielding behavior at a higher yield strength, but showed limited ductility, elongating only to 25%.

The most distinguishable effect of aging the material for 2 h at 200°C was the development of an 'easy flow' yield point. An increase in strength of aged 500b adversely corresponded to a serious reduction in tensile elongation. For 1000u, the specimens displayed prominent double yielding during early straining. Aging had an insignificant effect on the rest of deformation. The loss of tensile strength and ductility seen in 1000u could be attributed to

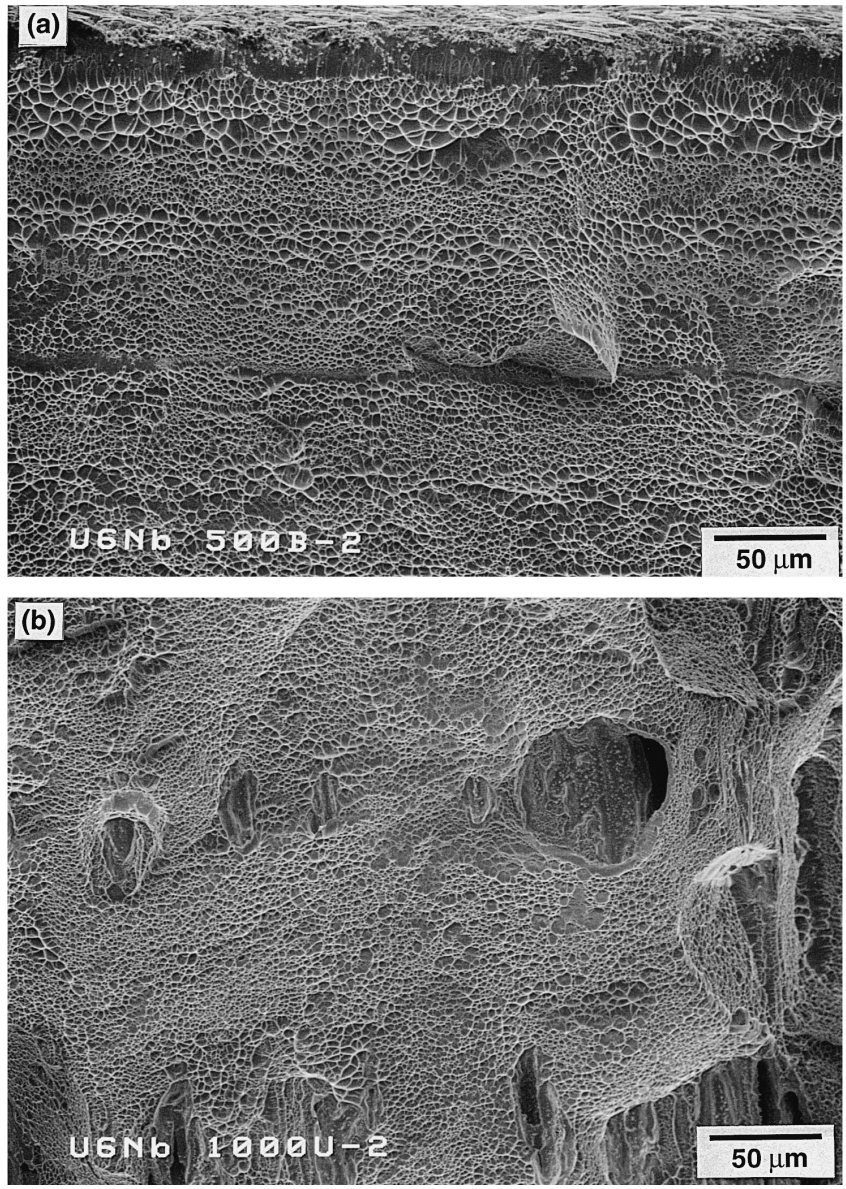

Fig. 8. SEM fractography of gamma quenched and aged PVD specimens tested at 25°C: (a) the fracture surface of a 500b specimen showing the variation in grain sizes through the thickness; (b) the fracture surface of a 1000u specimen showing a combination of homogeneous distribution of dimples with decohesion along the columnar boundaries.

the presence of microvoids causing a substantial reduction in columnar boundary strengths and leading to a decreased ability to deform plastically.

Testing at −40°C replicated some characteristics observed in both unaged and aged samples. The deformation behavior of the aged 500b, in particular, displayed a stress–strain curve similar to that of the as-quenched specimens, but at strength values increased by 20%. In addition, deformation at low temperatures increased average tensile elongation from 25% to 38%, indicating that there must be other deformation mechanisms operating at such temperatures. For the aged 1000u specimens, the subzero test temperature had little effect on the tensile elongation, which remained at 20%, but increased the strength values by some 20%.

Fig. 6(a) and (b) compare the effect of processing on the tensile deformation behavior of the gamma-quenched and aged PVD and wrought U–6% Nb alloy at 25°C and −40°C, respectively. A double yield phenomenon is seen in stress–strain curves and is more predominant for 1000u and the wrought alloy than for 500b. Despite columnar grain morphology, 1000u specimens displayed the highest strengths, as well as strain hardening behavior, compared to other PVD series and wrought material at both temperatures. Tensile properties of 500b at −40°C surpass those of the wrought material.

3.6. Fractography and fracture profiles

The difference in tensile ductility of the aged 500b specimens tested at 25°C and at −40°C can be clearly seen in Fig. 7. Compared to the 25°C tested specimen broke in shear (Fig. 7(a)), the −40°C tested specimen broke in a multi-faceted fracture, indicating sufficient resistance to deformation and to subsequent fracture (Fig. 7(b)). At a higher magnification, the effect of microbanding is quite apparent, where the variation in the dimple size corresponded to the band width (Fig. 8(a)). The size of these dimples was as fine as 3 μm, but they lacked the depth. From dimples observed in the fracture surface it may be deduced that failure may have occurred by transgranular fracture of subgrains.

Fig. 8(b) shows the fracture surface of the 1000u specimen tested at 25°C. The fracture mode consisted of a mixture of homogeneous distribution of dimples with decohesion along the columnar boundaries. The contribution of these microvoids to premature failure is evident in a cross-section of fractured 1000u specimen tested at 25°C (Fig. 9). Under tensile loading, microvoids increased in

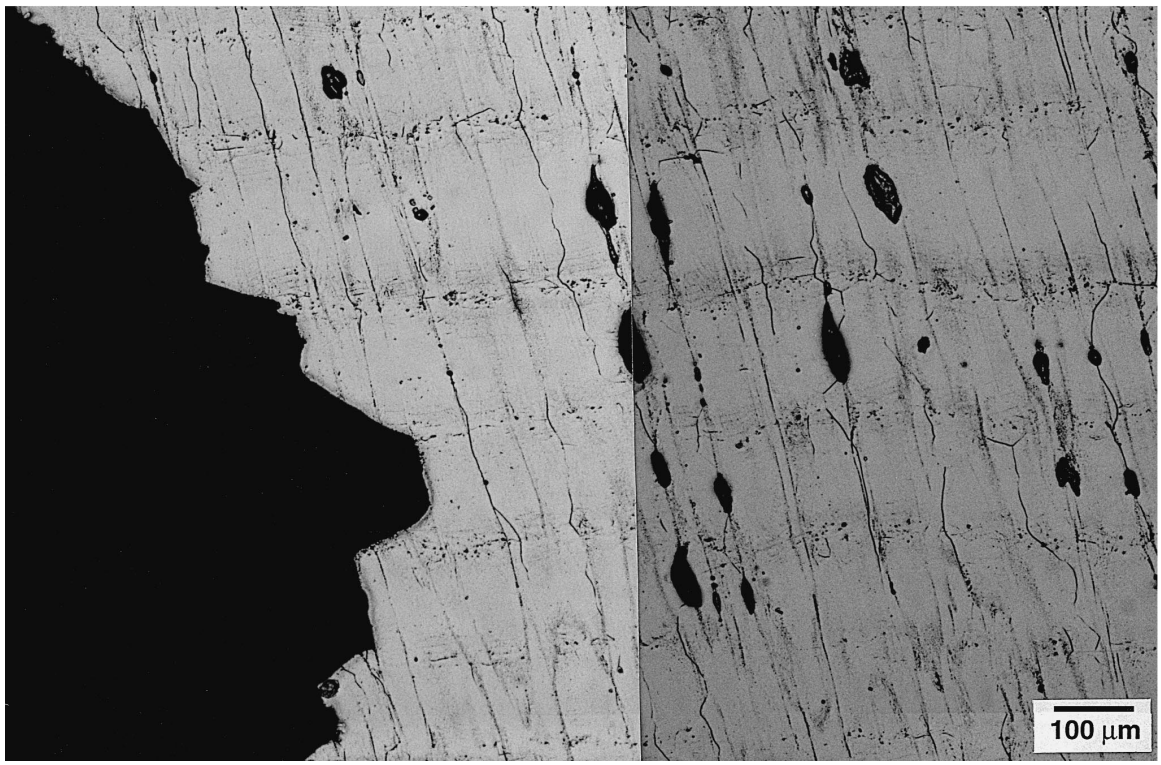

Fig. 9. A cross-sectional view of fractured 1000u specimen, showing the ability of columnar grains to deform and the microvoids contribution to crack propagation.

size and nucleated more cracks along the same faceted boundary, providing an easy linkage for a crack to propagate through the thickness. However, the figure also indicates that there was sufficient strength present in the columnar boundaries to resist crack propagation and to alter crack directions. As a result, a crack had to shear across several grains prior to fracture.

4. Conclusions

The PVD process conditions used in this study have produced a U–6% Nb alloy with two unique microstructures. We can conclude that grain morphology of PVD U–6Nb alloy was primarily determined by the PVD process itself and that microbanding intensity was primarily determined by temperature, which in turn controlled the diffusivity of Nb and U.

Very fine, equiaxed grain specimens of the heat treated 500b displayed increased strengths and ductility as the test temperature decreased from 25°C to −40°C, exceeding the tensile properties of the wrought material. The columnar structure present in the 1000u did not adversely affect the tensile deformation. Moreover, prior to failure, 1000u displayed a higher tensile strength and strain hardening characteristics that were observed in comparable wrought material. Hence, the PVD process has been shown to be an excellent alternative to the wrought process.

Acknowledgements

A.J. Sunwoo is grateful to Professor T.B. Massalski for technical advice and input. The authors would like to thank T.M. Anklam and T.A. Biesiada Jr. for providing the PVD material. This work was performed under the auspices of the US Department of Energy by the Lawrence Livermore National Laboratory under Contract No. W-7405-Eng-48.

References

[1] C.J. Long, T.M. Anklam, R.B. Addis, T.S. Chow, Lawrence Livermore National Laboratory Report UCRL-JC-122016 (1995).
[2] A.N. Holden, Physical Metallurgy of Uranium, Addison-Wesley, MA, 1958, p. 250.
[3] M. Anagnostidis, M. Colmbie, H. Monti, J. Nucl. Mater. 11 (1964) 67.
[4] K. Tangri, D.K. Chaudhuri, J. Nucl. Mater. 15 (1965) 278.
[5] J.J. Rechtien, R.D. Nelson, Metall. Trans. A 4 (1973) 2755.
[6] K.H. Eckelmeyer, A.D. Romig, L.J. Weirick, Metall. Trans. A 15 (1984) 1319.
[7] R.F. Bunshah, R.S. Juntz, J. Vac. Sci. Technol. 9 (1972) 404.
[8] O.H. Krikorian, Lawrence Livermore National Laboratory Report UCID-18258 (1975).
[9] R.A. Vandermeer, J.C. Ogle, W.G. Northcutt Jr., Metall. Trans. A 12 (1981) 733.
[10] D.H. Wood, J.W. Dini, H.R. Johnson, Lawrence Livermore National Laboratory Report UCRL-87267 (1982).